

Studies on candidate approaches for satellite-ground laser communications

Yoshihisa Takayama, Yoshisada Koyama, Hideki Takenaka, Hiroo Kunimori and Morio Toyoshima

National Institute of Information and Communications Technology

Tokyo, Japan

takayama@nict.go.jp

Abstract— Activities to perform satellite-ground laser communications and approaches to simply the optical ground station are introduced. We show a small optical transponder for a small satellite, the analysis of cloud distribution to estimate the possibility of satellite-ground links for the site diversity scheme, and the estimation of performance of a simplified optical ground station. As an unconventional idea, we describe an approach to employ the negative refractive behavior for passive beam coupling.

Keywords- *small optical transponder, SOTA, site diversity, optical ground station, OGS, negative refractive behavior.*

I. INTRODUCTION

Recently the successful demonstrations of the inter-satellite communications and the satellite-ground communications attract attentions as one of the promising technologies to provide broadband and long distance communications [1-6]. In the field of satellite applications, the use of small satellites seems to be one of the interesting topics. The relatively short development period of a small satellite enables us to have ideas and plans to utilize sophisticated technologies such as a high resolution imaging, wideband measurement, and so on.

The survey of the earth observation satellites reports that the data transmission is less than 1Mbps if the mass of a satellite is less than 100kg in most cases [7]. Thus, one of our challenges is to provide a small optical communication terminal for a small satellite, where the data rate is more than 1Mbps and the mass of the satellite is about 50kg. The optical communication terminal is named as the Small Optical Transponder (SOTA) [8].

When we look at an optical ground station (OGS) for satellite-ground laser communications, selection of the locations of OGSs is important to improve the availability of the satellite-ground link with the site diversity scheme. Therefore we have estimated the cloud distribution over the Japan area to find a set of sites that mutually shows small correlation in the cloud distribution tendencies [9].

Concerning the functions such as gimbals, fast steering mirrors and sensors in the optical system of OGS, one of our activities is to look for a way to simplify the OGS's structure. The study to use an optical fiber of a large core diameter to couple the received beam is an example, where the degree of the arrival angle of the signal beam has been studied to estimate the coupling efficiency of the received signal beam without the fast steering mirror. In other activities, we have

proposed an unconventional method to couple the received beam into a small detector or an optical fiber of a small core diameter, where an optical device of periodical structure has been used to obtain the negative refractive behavior.

In this work, we introduce our activities concerning the small optical transponder to be mounted on a satellite, the site selection for optical ground stations, and the estimation of potential of a simplified OGS. Besides, an idea to improve the coupling efficiency of light is described as an unconventional approach.

II. OPTICAL COMMUNICATION EQUIPMENT ONBOARD

A. Small Optical Transponder (SOTA)

The optical part of SOTA is shown in Fig. 1. The total mass including the optical and the electrical parts are 6.2kg. The dimensions of the optical part including the fork mount gimbals are (W)178mm, (D)117mm, and (H)278mm. SOTA is equipped with three wavelengths laser sources of 0.8 μ m, 0.98 μ m and 1.5 μ m, respectively. They are labeled as Tx1 for 0.98 μ m, Tx2 and Tx3 for 0.8 μ m and Tx4 for 1.5 μ m. With those wavelengths, the conventional laser communications and a basic experiment for the quantum key distribution are planned [8].

The diameter of the acquisition and the tracking sensor is 23mm and the diameter of the main telescope for Tx4 is 50mm. For the downlink, SOTA selects one of the two data rates of 1Mbps and 10Mbps. The average transmission powers of the downlinks are 24.3dBm for Tx1, and 16.0dBm for Tx4, respectively. Due to the limitation of the power consumption, Tx1 and Tx4 should be turned on exclusively. SOTA chooses either Tx1 or Tx4 for the downlink to perform the conventional laser communication demonstrations, while, in the basic experiment for the quantum key distribution, Tx2, Tx3 and Tx4 are turned on simultaneously. The downlink lasers of Tx1 and Tx4 are modulated with a pseudo noise code or image data of camera installed in the satellite. Besides, the coding technologies such as the Reed-Solomon and LDGM can be superimposed for error correction.

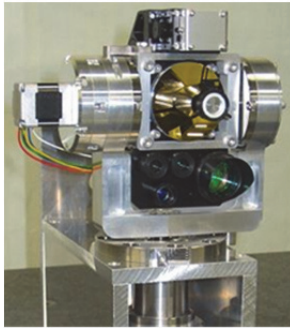


Figure 1. Optical part of SOTA protoflight model

III. OPTICAL GROUND STATION

A. Selection of location

When the satellite-ground laser communications are carried out, the blockage of the optical paths by the clouds is a problem to be avoided. For the avoidance of the cloud blockages, we are looking at the site diversity scheme where the plural optical ground stations mutually connected through the terrestrial communication networks are used. The laser communication link could be established if at least one of the optical ground stations under the clear sky can access to the satellite.

To select the candidate locations for the optical ground stations, the cloud distribution is calculated by using images taken by a meteorological satellite. The sample image is given in Fig. 2, where the northern part of Japan is found in the middle of the picture. The detection wavelength ranges between $10.3\mu\text{m}$ and $11.3\mu\text{m}$. For our study, such images are prepared for one year, from June 1 in 2007 to May 31 in 2008. We select 100 sites in Japan area and compute each image to extract the pixel values at all the selected points. Although the atmospheric characteristics such as the transparency are beyond the considerations due to the approach based on the pixel values of the images, the evaluation gives us good insight to find the combination effect of the multiple ground stations.

The numerical correlations of the sequentially extracted pixel values at Tokyo with the ones at the other locations are computed by the Pearson product-moment correlation coefficient given as

$$r = \frac{\frac{1}{N-1} \sum_{i=1}^N (X_i - \bar{X})(Y_i - \bar{Y})}{\sqrt{\frac{1}{N-1} \sum_{i=1}^N (X_i - \bar{X})^2} \sqrt{\frac{1}{N-1} \sum_{i=1}^N (Y_i - \bar{Y})^2}} \quad (1)$$

where N is the total number of the processed images, X_i means the pixel value at Tokyo in the i -th image, Y_i means the pixel value at a certain selected location in the i -th image, \bar{X} and \bar{Y} are the average of X_i and Y_i , respectively.

The correlation coefficient is given in Fig. 3, where the selected 100 cities are arranged along the abscissa mostly from the north of Japan to the south. In the figure, four candidate cities are shown for reference. Those locations are indicated in Fig. 4. In Fig. 3, the correlation coefficient labelled Tokyo is 1 as the self-correlation. Here we find that the correlation

coefficient with Naha is almost 0, which implies that the cloud distribution of the city is independent to the one of Tokyo. Therefore if we select one city to combine with Tokyo in order to avoid the cloud blockages, Naha would be an effective location.

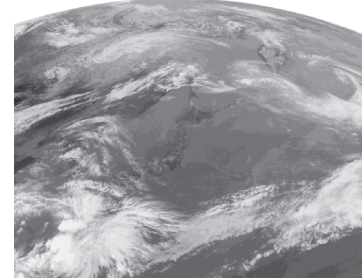


Figure 2. Sample image used for calculation.

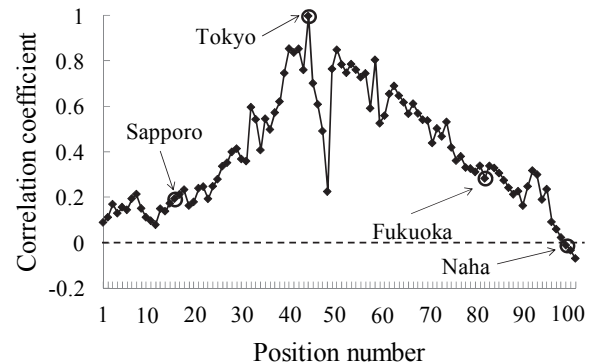


Figure 3. Correlation coefficient on cloud distribution.

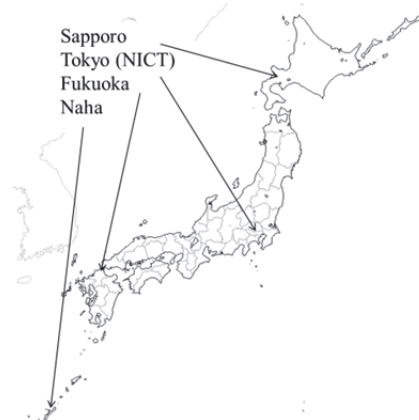


Figure 4. Candidate sites for OGSs

B. Simplified optical ground station

In most cases, laser communication terminals are equipped with the coarse pointing function, the fine pointing function and the point-ahead function as well as the transmission and reception functions of the signal beam. The terminals acquire and track the beam from the counter terminal by controlling the coarse pointing and the fine pointing functions, and the transmission direction of the signal beam is modified by the point-ahead function.

Here we consider a simplified optical terminal shown in Fig. 5 for OGSs, where the coarse pointing function of the optical antenna is equipped with the signal receiver and the beacon transmitter. The optical axis of the telescope is parallel to the direction of the beacon transmission. When we conduct the satellite-ground laser communications with such a simplified OGS, the performance is directly influenced by the atmospheric turbulences, the lack of point-ahead angle compensation, and so on. Those influences appear even if the optical terminal on a satellite is fully functional to transmit the signal beam toward the OGS in the ideal direction, because the transmission direction of the optical terminal onboard is determined by the arrival angle of light from the OGS.

Among the atmospheric influences, one of the dominant phenomena is the beam wander. Fig. 6 shows that the beacon beam from the OGS collected at the satellite is moving on the receiving plane of the optical terminal, where $\langle r_c^2 \rangle$ is a variance of the distance between the ideal center of the beacon illumination area with no atmospheric influences and the center of the illumination area affected by atmosphere. The angle variation caused by the beam wander is obtained as $\langle r_c^2 \rangle/L$, where L is the distance between the OGS and the satellite [10].

For computation, we assume that the orbit of the satellite is circular with the altitude 600km and the OGS locates within the orbit plane. In this case, the required point-ahead angle for OGS is about 20 μ rad at the elevation angle 0deg and increases up to 50 μ rad at the elevation angle 90deg. Besides, the angular fluctuation due to the beam wander is added to the point-ahead angle. By using the Hufnagel-Valley(H-V) model, the error angle caused by the beam wander and the point-ahead is obtained as shown in Fig. 7. Since the satellite is assumed to transmit the beam toward the ideal direction, the angular error in the beacon beam from the OGS directly affects the transmission direction of the signal beam of the satellite, and that is observed as the arrival angle error in the OGS.

The arrival angle error causes the spread of the exposed area of the received beam on the OGS receiving plane. The spread of the exposed area is proportional to the focal length of the OGS receiving optics. Here we assume that the ratio of the OGS telescope radius to the focal length is 0.1, and the results are shown in Fig. 8. Here the case with the point-ahead compensation and the case without the compensation are plotted.

The use of optical fibers provides easier handing of the optical setup than an optical setup where lenses and mirrors are arranged. Therefore, if we use an optical fiber to couple the light that the OGS receives from the satellite, the core area is required to be larger than the exposed area on the OGS receiving plane. A dotted line in Fig. 8 is drawn at 30 μ m of the spot wander range, for example, that intersects the plots at 0.07m and 0.4m on the transmission radius, respectively. Therefore, if a fiber with the core radius of 30 μ m is used in this OGS, the effective radius of the telescope is less than 7cm in the case without the point-ahead compensation and 40cm in the case of the point-ahead compensation.

Besides, the numerical aperture of the fiber should be taken into considerations to estimate the acceptable data rate. According to the geometrical optics, the acceptable bandwidth

of the fiber is computed and shown in Fig. 9, where the numerical aperture of the fiber is assumed as 0.2, and the fiber is the step index type with the refractive index of the core is 1.49 [11]. The acceptable bandwidth is a function of the length of the fiber as shown in Fig. 9.

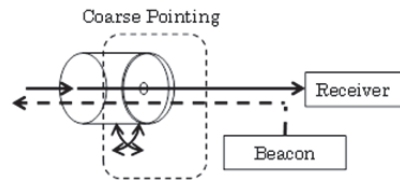


Figure 5. Simplified optical ground station

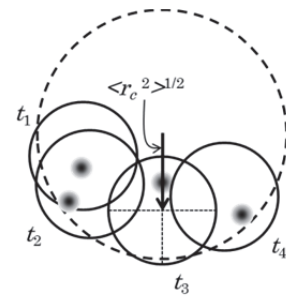


Figure 6. Beam wander

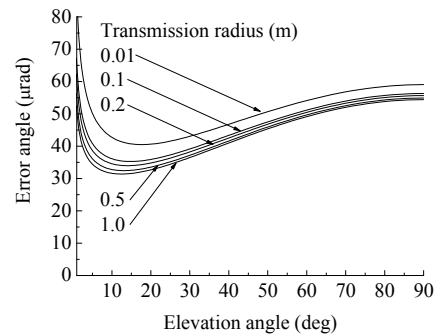


Figure 7. Beam wander angle

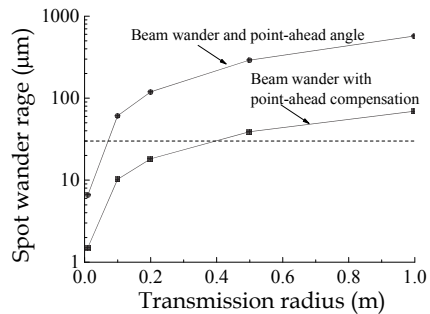


Figure 8. Spot wander range

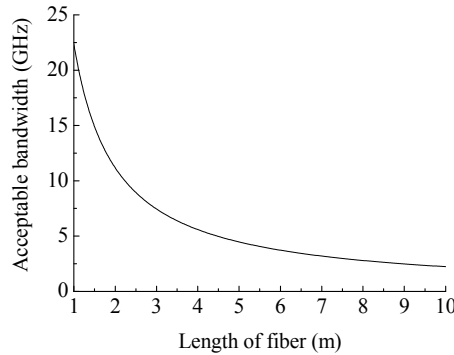


Figure 9. Acceptable bandwidth of a fiber.

C. Unconventional approach for coupling of received beam

It is known that a slab of a negative refractive index medium placed behind a focal point of a lens causes the rays exiting from the focal point A_f to gather again at the point A_b as shown in Fig. 10 [12]. For example, the ray denoted by the bold arrow labeled j_f goes into the slab from air, refracts toward a negative direction in the angular sense, and finally exits as the ray labeled j_b . When the boundaries of the slab are mutually parallel, the arrows j_f and j_b point in the same direction. Therefore, an optical detector accepting light at the position A_f can be replaced by the position at A_b to receive the light within the same numerical aperture. Here we note that the line connecting the point A_f and A_b is perpendicular to the boundaries of the slab.

This line of thought led us to consider an approach shown in Fig. 11, where the focal points of the light received by a telescope spread to the range W_f , but the range is reduced to W_b behind the negative refractive medium slab. Here, the propagation direction of each ray in front of and behind the medium remains the same if the boundaries in each case are mutually parallel. Therefore, all the rays can be coupled if an optical detector or a fiber with a diameter larger than W_b is put behind the medium [13].

For a material of the negative refractive behavior, we look at a photonic crystal of two-dimensional lattice structure as shown in Fig. 12. The rectangular rods with the cross section size $0.1d$ by $0.4d$ are arranged in a square where d is the distance of the neighboring rods. We assume d is equal to 0.51λ , λ is the wavelength of the light, and the refractive indices of the rods n_r and the background n_b are 3.35 and 1.55, respectively.

In Fig. 13, the material showing the negative refractive behavior has curved boundaries and the rays come out of three points A, B, and C within the width W_f at $x=0$. The distances between the neighboring points are normalized to 1. The boundaries b_1 and b_2 are segments of circles with the radius 30 and 28, respectively. The range W_f is reduced to W_b at $x=19$ with the reduction ratio of 37.5%. In the sample calculation, the recreated focuses behind the crystal seems to become blurred but the propagation directions of the rays are almost the same as the ones in front of the crystal.

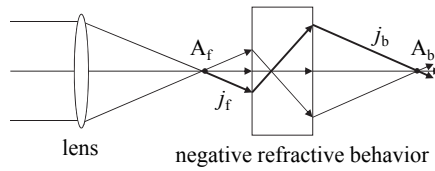


Figure 10. Propagation of light caused by the negative refractive behavior.

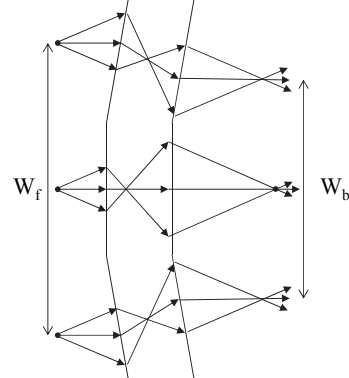


Figure 11. Spatial shift of focal points

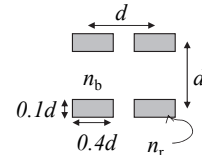


Figure 12. Photonic crystal of lattice structure

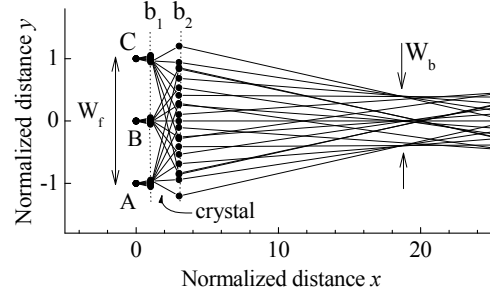


Figure 13. Reduction of the range that all the beams passes through

IV. CONCLUSIONS

We have introduced our activities concerning satellite-ground laser communications. As the equipment on a satellite, the small optical transponder SOTA is introduced first. As the activities on the optical ground stations, the cloud distribution analysis for the site selection of optical ground stations has been carried out. The calculation has found a combination of sites with almost no correlation even within Japan area. For the estimation of potential of a simplified OGS, the use of large core diameter is studied. Besides, an idea to utilize the negative refractive behavior has been described to gather the light without expanding the propagation angles.

References

- [1] T. TolkerNielsen, G. Oppenhaeuser, "In-orbit test result of an operational optical intersatellite link between ARTEMIS and SPOT4, SILEX," Proc. SPIE 4635, 2002, pp.1-15.
- [2] T. Jono, Y. Takayama, K. Shiratama, I. Mase, B. Demellenne, Z. Sodnik, A. Bird, M. Toyoshima, H. Kunimori, D. Giggenbach, N. Perlot, M. Knapek, K. Arai, "Overview of the inter-orbit and the orbit-to-ground lasercom demonstration by OICETS," Proc. SPIE, 6457, 2007, pp. 645702-1-10.
- [3] M. Toyoshima, H. Takenaka, C. Schaefer, N. Miyashita, Y. Shoji, Y. Takayama, Y. Koyama, H. Kunimori, S. Yamakawa, E. Okamoto, "Results from phase-4 Kirari optical communication demonstration experiments with the NICT optical ground station (KODEN)," AIAA ICSSC3.4.2, 2009.
- [4] N. Perlot, M. Knapek, D. Giggenbach, J. Horwath, M. Brechtelsbauer, Y. Takayama, T. Jono, "Results of the Optical Downlink Experiment KIODO from OICETS Satellite to Optical Ground Station Oberpfaffenhofen (OGS-OP)," Proc. SPIE, 6457, 2007, pp. 645704-1-8.
- [5] B. Smutny, R. Lange, H. Kämpfner, D. Dallmann, M. Gregory, G. Mühlnikel, "High Data Rate Optical Inter-Satellite Links," Proc. ICSOS, 1, ICSOS2009-2, 2009, pp. 1-5.
- [6] K. E. Wilson, J. M. Kovalik, A. Biswas, M. W. Wright, W. T. Roberts, Y. Takayama, S. Yamakawa, "Preliminary results of the OCTL to OICETS optical link experiment (OTOOLE)," Proc. SPIE 7587, 2010, pp. 758703-1-13.
- [7] M. Toyoshima, H. Takenaka, Y. Shoji, Y. Takayama, Y. Koyama, M. Akioka, "Small Optical Transponder for Small Satellites", Proc. CSNDSP 2010, OWC-9, 2010, pp. 558-561.
- [8] Y. Takayama, M. Toyoshima, Y. Koyama, H. Takenaka, M. Akioka, K. Shiratama, I. Mase, O. Kawamoto, "Current development status of Small Optical TrAnsponder (SOTA) for satellite-ground laser communications," Proc. SPIE 8246, 2012, pp. 824607-1-7.
- [9] Y. Takayama, M. Toyoshima, Y. Koyama, H. Takenaka, M. Akioka, K. Shiratama, I. Mase, O. Kawamoto, "Development of small optical transponder for satellite-ground laser communication demonstrations", 17th Ka and BroadBand Communications Conference, 2011, pp. 1-6.
- [10] L. C. Andrews, R. L. Phillips, R. J. Sasila, R. R. Parenti, "Strehl ratio and scintillation theory for uplink Gaussian-beam waves: beam wander effects," Opt. Eng. 45, 7, 2006, pp. 076001-1-12.
- [11] G. Keiser, *Optical fiber communications*, 3rd edition, McGraw-Hill Higher Education, Singapore, 2000, Chap. 3.
- [12] J. B. Pendry, "Negative refraction makes a perfect lens", Phys. Rev. Lett. 85, 18, 2000, pp. 3966-3969.
- [13] Y. Takayama, W. Klaus, K. Shinohara, "Passive approach to expand the field of view of receivers for free-space laser communications", Opt. Eng. 44, 5, 2005, pp. 0560031-0560038.